



CMT Twin welding-brazing of aluminum to titanium

Wanghui Xu¹ · Wenhui Wang^{2,3} · Qingfu Yang¹ · Jinye Xiong¹ · Lixin Zhang² · Huan He²

Received: 3 December 2021 / Accepted: 2 March 2022 / Published online: 7 March 2022
© International Institute of Welding 2022

Abstract

A cold metal transfer (CMT) Twin welding-brazing technique was applied to Ti/Al dissimilar metals for the first time. Significant improvements in intermetallic compound (IMC) suppression and joint strength were obtained. Compared with the normal CMT, the reasonable range of the welding heat input was extended by 15.4%, the IMC thickness was further suppressed to 0.53 μm , the maximum tensile strength of the joint was up to 297 MPa, and the fracture position was transferred from the IMC layer to the base aluminum, by employing the CMT Twin. The serrated IMC was identified to be $\text{Ti}(\text{Al}, \text{Si})_3$ by TEM and evenly distributed at the interface layer. Whether for the common single-wire CMT or CMT Twin, with decreasing heat input, the IMC thickness decreased, and the joint strength increased. The CMT Twin shows significant advantages over the traditional single-wire CMT in terms of a higher welding speed, lower heat input, thinner IMC thickness, and higher joint strength on the joining of incompatible dissimilar alloys.

Keywords Aluminum · Titanium · Intermetallic · CMT Twin · Welding-brazing

1 Introduction

Lightweight alloys have been widely used in various industries for weight and cost reduction purposes. Titanium and aluminum alloys rank among the most important lightweight alloys because they provide excellent performance in many applications [1, 2]. Titanium alloys provide a high strength/weight ratio, superior corrosion resistance, and the ability to perform at high temperatures. Aluminum alloys are versatile in automobile industry applications where low cost, lightweight, and good plasticity are required. By appropriately

joining the two alloys, a joint with complementary advantages of them will be obtained, which has a huge market in aerospace and other application fields [3, 4]. However, it is generally accepted that obtaining a good joining of Ti/Al is hindered by metallurgical incompatibility, the differences of their physical properties, and dominantly by the formation of brittle intermetallic compounds (IMCs) [5, 6].

Although the formation of the IMCs is necessary for the metallurgical joining of aluminum to titanium, their thickness must be controlled. Traditional fusion welding experiences a reaction between liquid aluminum and liquid titanium, which makes it impossible to avoid the massive formation of the brittle IMCs [7]. Solid-state joining processes such as explosive welding [8], diffusion welding [9], friction welding [10], and friction stir welding [11–13] rely on solid-state reactions and low-temperature thermal cycles, which can effectively suppress the IMCs. Welding-brazing processes skillfully avoid the difficulties caused by the different melting points of the two compounds, which has great advantages in joining dissimilar metals. Many joints were obtained by welding-brazing with arc [14–18], laser [19–22], and electron beam [23].

However, it is possible but more difficult to control the IMCs in the Al/Ti welding-brazing process based on a solid–liquid interface reaction in a few seconds. Generally, three dominant options could be employed to control

Recommended for publication by Commission II - Arc Welding and Filler Metals

✉ Huan He
welderhehuan@yahoo.com

¹ Guangdong Province, China-Ukraine Institute of Welding, Guangdong Academy of Sciences, No. 363, Changxing Road, Tianhe District, Guangzhou 510650, People's Republic of China

² School of Nuclear Equipment and Nuclear Engineering, Yantai University, No. 30, Qingquan Road, Laishan District, Yantai 264005, People's Republic of China

³ School of Materials Science and Engineering, University of Science and Technology Beijing, NO. 30, Xueyuan Road, Haidian District, Beijing 100083, People's Republic of China

the IMC growth in the above system. The first option is to employ appropriate alloying elements in base metals or fillers to adjust the interfacial reaction [24–28]. Another choice is to add an intermediate layer to hinder the mutual diffusion of atoms, such as Zn [29] and Nb [30]. Additionally, the growth of the IMCs can be controlled effectively by decreasing the heat input during Al/Ti welding. Yufeng Zhang et al. used a MIG/TIG double-sided arc welding-brazing to control the heat input, suppress the IMC layer to 2–6 μm , and increase the joint strength to 240.3 MPa [31]. Rui Cao et al. applied a low heat input welding technique—cold metal transfer (CMT) to Al/Ti joining for the first time [32]. Ming Gao et al. employed laser-CMT hybrid welding to reduce the heat input and control the IMC thickness, but the IMC thickness along the vertical direction was inhomogeneous [33].

Most previous studies on CMT joining of Ti/Al dissimilar alloys were based on the traditional single-wire CMT. Although these works have indicated a promising effect on controlling welding heat input, the performance of the Al/Ti joints still cannot fully meet the requirements of all the application fields. As an upgrade of the single-wire CMT, a CMT Twin technique based on the setup of two power sources, one torch, and two insulated contact tips (“Lead” and “Trail”) was developed. The CMT and pulsed processes can be combined, and better self-regulated than ever before can be accomplished. Especially, CMT Twin welding has more significant advantages than traditional single-wire CMT welding for joining aluminum to titanium, such as less heat input, independent adjustments of fillers, and welding parameters of the two incompatible alloys.

In this study, the CMT Twin process is applied to Ti/Al butt welding-brazing to study the interfacial IMC layer and joint strength, compare the mechanical properties of the joints obtained by the traditional single-wire CMT and CMT Twin processes, and discuss the relationship among the welding parameters, microstructure, and joint properties.

2 Materials and methods

The TC4 titanium alloy and 5083 aluminum alloy sheets used in the experiment were 3 mm \times 100 mm \times 60 mm in size, and a 45° single V-groove was cut on both sides of the two sheets. The filler metal was an ER4043 aluminum welding wire with a diameter of 1.2 mm. According to the data sheets provided by the producer, the chemical compositions of the materials are listed in Table 1. The shielding gas used was 99.999% ultra-high purity argon produced by the Air Products company. Before welding, oxide films on the surfaces of the alloys were cleaned by brush and acetone, and then, a 0.2–0.5-mm-thick non-corrosive KAlF₄ flux was coated on the grooves as well as on the face and back surfaces of the titanium alloy.

A schematic of the CMT Twin welding-brazing process is illustrated in Fig. 1. Twin Fronius TPS CPT power sources and a KUKA arc welding robot were employed in this study. A groove gap of 1 mm was reserved between the aluminum and titanium alloys. The welding torch kept vertical to the plates. There was an angle of approximately 7° between the two wires in the CMT Twin process.

Table 1 Chemical composition of the base and filler metals (wt%)

Elements	Ti	Al	Fe	V	Mg	Mn	Si	Cu
TC4	Bal	5.50~6.75	≤ 0.3	3.5~4.5	-	-	-	-
5083	0.15	Bal	0.4	-	4.0~4.9	0.4~1.0	0.4	0.1
ER4043	0.20	Bal	0.8	-	0.05	0.05	4.5~6.0	0.3

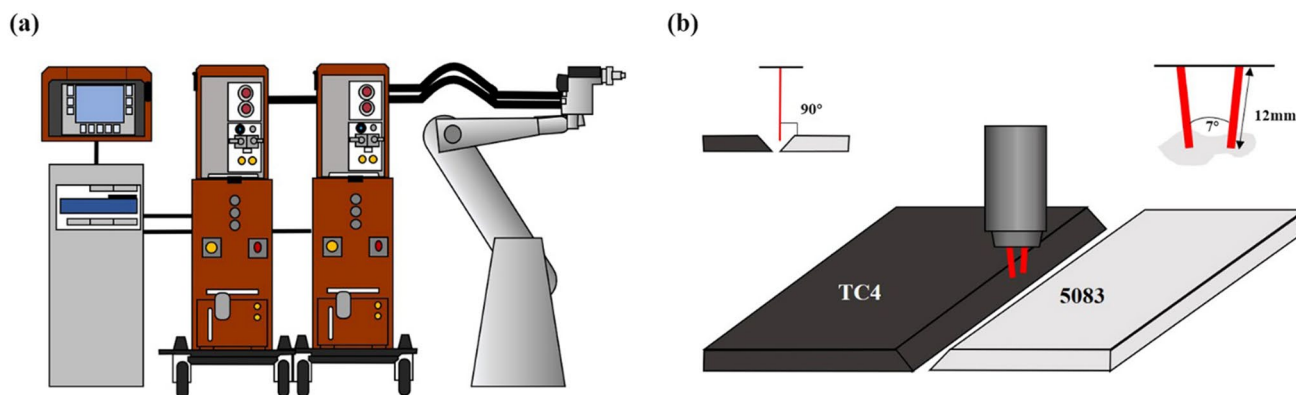


Fig. 1 Schematic of the CMT Twin welding-brazing process: **a** welding system, **b** welding-brazing process

The CMT welding process was applied in the experiment, and a twin CMT mode was performed for welding. In one motion cycle, the front wire performs a jet transition in the first period of the cycle. In the next period, the droplet transfer is carried out by mechanical wire pullback, which is a typical CMT mode. The rear wire is in the CMT mode throughout the entire welding cycle. The welding robot controls the welding wire to start the arc at the beginning of the path and then moves to the end of the path along the preset track. During the welding, the two welding wires cooperate with each other under the regulation of the control system to complete the welding. The classical linear energy equation (single-wire CMT, $Q=IU/v$; CMT Twin, $Q=2*IU/v$) was used to calculate the welding heat input.

After welding, one metallographic and three tensile test specimens were cut from each weld plate by wire electrical discharge machining. The macrostructure samples were polished to mirror-like surface aspects. Then the macrostructure of the joint was inspected using a Suzhou Huiguang HSH-200C plane test microscope. The metallographic structure was observed using a Zeiss Ario Imager M2m digital metallographic microscope after the samples were etched in Keller's reagent for 5–10 s. The microstructure of the interfacial layer was observed using an ultra-high resolution field emission scanning electron microscope (FEI-Nova Nano SEM 430, The Netherlands). TEM samples of approximately $4\ \mu\text{m} \times 4\ \mu\text{m} \times 0.09\ \mu\text{m}$ were prepared from the cross-section. The IMC at the interface was examined with a transmission electron microscope (FEI Talos F200X) equipped with an energy dispersive spectrometer (EDS). The reinforcement on the specimens was retained, and tensile tests were conducted using the SHIMADZU AG-IC universal testing machine.

3 Results

3.1 Welding parameters

The welding parameters of the CMT Twin and single-wire CMT were determined by pre-experiments, as shown

in Table 2. For Ti/Al CMT welding-brazing, there is a reasonable welding heat input range that can obtain an acceptable weld formation, as illustrated in Fig. 2. Once beyond this range, excessive heat input will lead to the melting of titanium base metal and generate massive brittle IMCs, while inadequate heat input cannot guarantee the melting of the aluminum base and filler metals. Employing the CMT Twin extended the range of heat input by 15.4% and made the range shift to a negative direction. The expansion and shift of the welding heat input window help achieve a more stable welding process and a lower interface temperature.

3.2 Macrostructure and microstructure

Visual inspection was performed on the samples. No obvious weld defects were observed in Fig. 3a. Figure 3b presents a typical cross-sectional view of the welding-brazing joint with the CMT Twin. Reinforcements at the face and root of the joint were observed. The aluminum alloy, which had a low melting point ($570\ ^\circ\text{C}$), was fused and mixed with the liquid filler metal to produce the welded seam with an

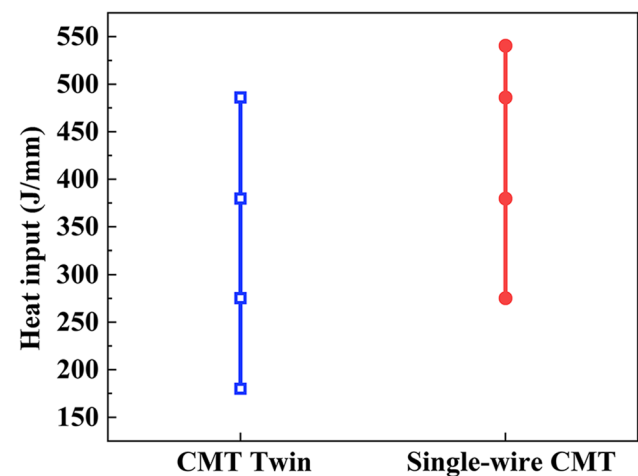


Fig. 2 Ranges of welding heat input for different welding methods

Table 2 Welding parameters

Method	Wire feed rate (m/min)	Welding speed (m/min)	Welding current (A)	Voltage (V)	Heat input (J/mm)
CMT Twin	3	0.4	40	15.0	180.0
	4	0.4	57	16.1	275.3
	5	0.4	74	17.1	379.6
	6	0.4	90	18.0	486.0
Single-wire CMT	4	0.2	57	16.1	275.3
	5	0.2	74	17.1	379.6
	6	0.2	90	18.0	486.0
	6.5	0.2	99	18.2	540.5

obvious fusion line, while the titanium alloy, which had a high melting point (1650 °C) and remained in the solid state during the welding-brazing process, was wetted by the liquid aluminum and reacted with it at the interface. Metallography of the fusion welding area of the aluminum alloy and the brazing area of the titanium alloy in this cross-sectional area are shown in Fig. 3c and d, respectively. A uniform IMC layer can be observed in the Ti/welded seam interface in Fig. 3d.

The TEM microstructure of the IMC layer is shown in Fig. 4. The FIB selection area is shown in Fig. 4a and b. From Fig. 4c, the compound on the interface layer between the titanium alloy and the weld metal is a monolayer, growing from the titanium side into the weld bead in an irregular serrated shape. Based on the TEM diffraction results in Fig. 4c, the IMC is identified as a tetragonal TiAl_3 phase with the lattice parameters of $a=0.3853$ nm and $c=0.8584$ nm [34].

The composition of the intermetallic layers was measured using EDS of the TEM foils and is summarized in Table 3. The results show that a small quantity of Si is contained in the IMC. The IMC was thus determined to be $\text{Ti}(\text{Al}, \text{Si})_3$.

3.3 Effect of heat input on IMC

The SEM images of the IMCs with different welding heat inputs are shown in Fig. 5. When the heat input is

relatively low, the interface is a large smooth plane. As the heat input increases, the interface gradually evolves into a serrated shape composed of many small planes with different inclination angles.

The thicknesses of the IMCs with varying heat inputs are illustrated in Fig. 6. The average thicknesses of the IMCs and standard deviation were calculated according to three different positions on the same specimen interface. With an increase of welding heat input from 180.0 to 486.0 J/mm, the IMC thickness at the CMT Twin welding interfaces increased constantly from 0.53 to 2.12 μm . Similarly, the thickness of the IMCs obtained by the single-wire CMT also increased from 1.83 to 3.22 μm with increasing heat input. However, under the same heat input, the IMCs obtained by the CMT Twin are thinner than those obtained by the single-wire CMT.

3.4 Mechanical properties

The results of tensile tests with and without reinforcement are shown in Fig. 7. The error bars in the Fig. 7 represent the standard deviation calculated from the tensile strength of three parallel specimens. For the joints with reinforcement, the tensile strength by CMT Twin decreased from 297 to 259 MPa, while the strength by single-wire CMT reduced from 218 to 155 MPa with increasing heat input. On the other hand, for the joints without reinforcement, the strength by CMT Twin decreased from 258 to 189 MPa, while the

Fig. 3 Macroscopic and microscopic images of the Ti/Al butt joint: **a** top view of the joint, **b** transverse cross section, **c** metallography of position 1, **d** metallography of position 2

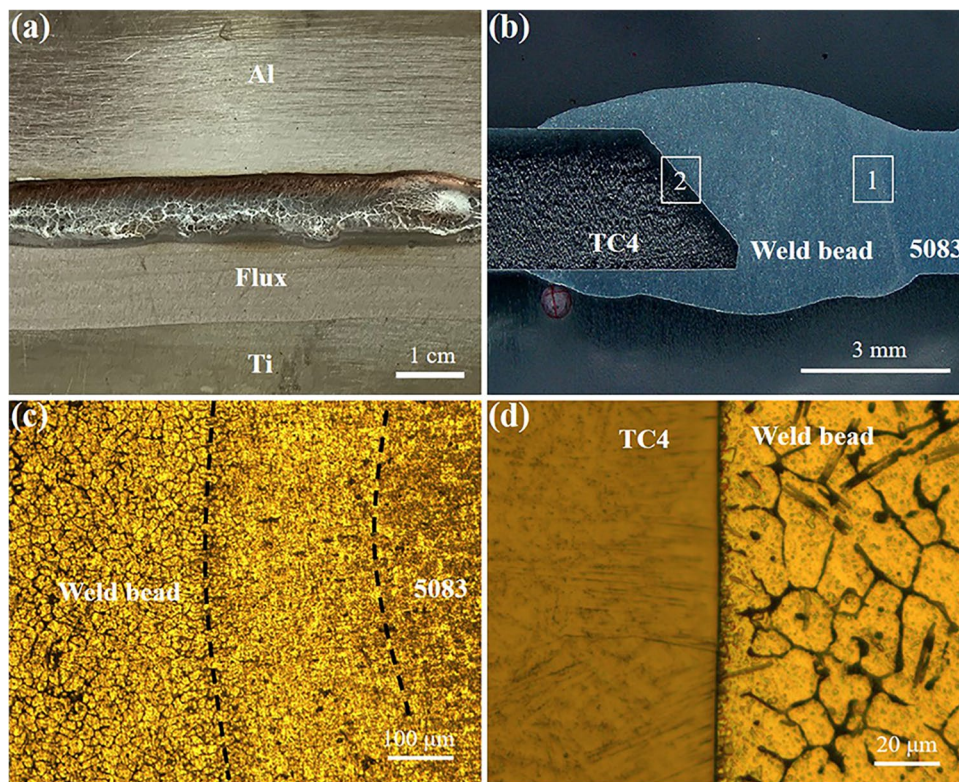
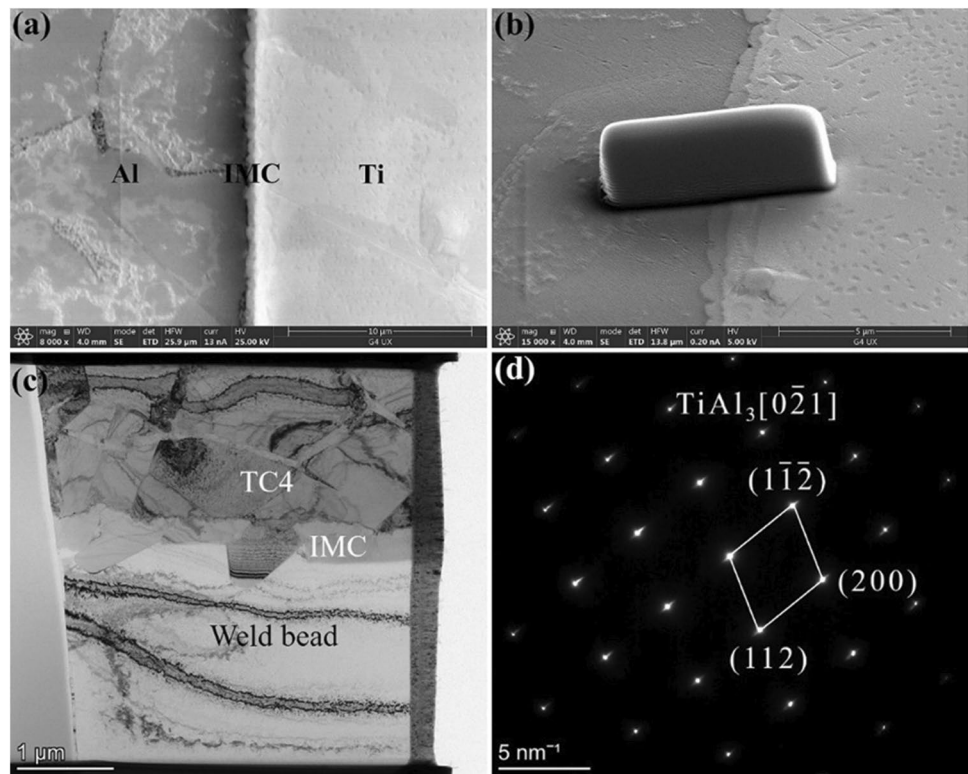


Fig. 4 IMC morphology and diffraction spots: **a** micrograph of the interface layer, **b** FIB sample preparation selection area, **c** TEM morphology, **d** TEM diffraction spot of $TiAl_3$



strength by single-wire CMT reduced from 219 to 119 MPa with increasing heat input. The tensile strength of the joints obtained by CMT Twin welding is higher than that of single-wire CMT in both cases with and without weld reinforcement. The maximum strength of the CMT Twin joint is 32% higher than that of single-wire CMT.

The microfracture profiles of the joints are shown in Fig. 8. First, for the joint with a relatively low tensile strength, the fracture originated at the root of the interface layer and extended to the weld. Furthermore, for the joints with higher strength, the crack evolved along the weld close to the fusion line. Finally, for the joint with the highest strength, fracture occurred at the base aluminum alloy.

3.5 Relationship between IMC thickness and joint strength

Figure 9 presents the relationship between the IMC thickness and tensile strength. The tensile strength decreases significantly with increasing IMC thickness. Joints with or without reinforcement show the same trend. When the IMC thickness is 0.53 μm , the tensile strength of the joint reaches a maximum of 297 MPa. The fitting results of the strength

Table 3 Analysis of EDS (at%)

Elements	Al	Si	Ti
	65.2	7.93	26.8

variation are summarized in Table 4. The absolute slope values of the CMT Twin fitting lines are smaller than the values of the single-wire CMT, indicating that the decreasing speed of the joint strength with increasing IMC thickness obtained by the CMT Twin is slower than that of the single-wire CMT.

4 Discussion

4.1 Microstructure and phase identification

In this work, a dominant layer ($TiAl_3$) between aluminum and titanium was observed. There are other IMCs, such as Ti_3Al , $TiAl$, $TiAl_2$, and Ti_2Al_5 , that may be present during the process but are not found in the final microstructures. Referring to the calculation results, the Gibbs energy of $TiAl_3$ is lower than that of $TiAl$ and Ti_3Al and higher than that of $TiAl_2$ and Ti_2Al_5 [35, 36]. Although the compounds $TiAl_2$ and Ti_2Al_5 have lower free energies of formation than $TiAl_3$, $TiAl_3$ is still the dominant IMC layer at the joining interface. Raman and Schubert may explain this phenomenon that is the formation of $TiAl_2$ and Ti_2Al_5 depends on the formation of $TiAl$ as one of the starting phases [37]. Moreover, when the welding heat input was high enough, the IMC at the interface shifted from a single $TiAl_3$ phase to $TiAl + TiAl_3$ [31]. In this study, the formation of the $TiAl$

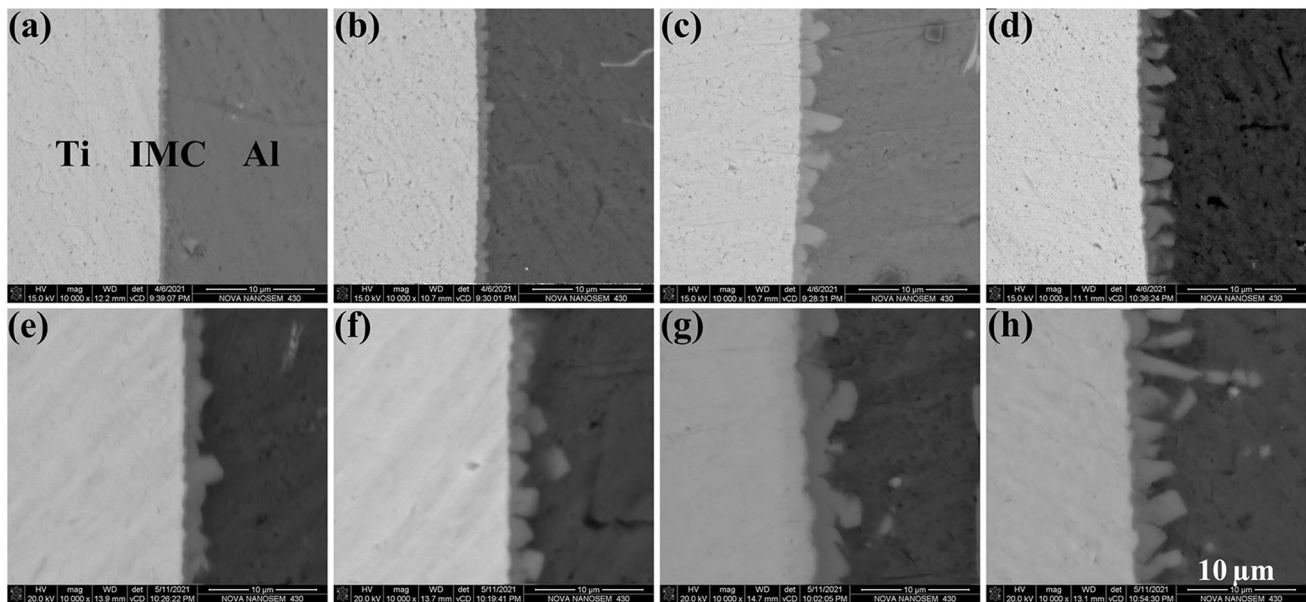


Fig. 5 SEM images of the IMCs under different welding heat inputs with CMT Twin (a–d) and single-wire CMT (e–h): a 180.0 J/mm, b 275.3 J/mm, c 379.6 J/mm, d 486.0 J/mm, e 275.3 J/mm, f 379.6 J/mm, g 486.0 J/mm, h 540.5 J/mm

was suppressed, possibly due to the effective control of the welding heat input by the CMT Twin welding technique, presenting a single thin layer of TiAl_3 .

On the other hand, based on the composition of the intermetallic layer from the EDS, the IMC can also be expressed as $\text{Ti}(\text{Al}, \text{Si})_3$. For the Ti–Al–Si system, since the silicon and aluminum atoms are very similar in atomic radius (111 pm and 118 pm, respectively [38]) and can easily undergo substitution reactions, $[\text{Si}] + \text{TiAl}_3 \rightarrow \text{Ti}(\text{Si}_x\text{Al}_{1-x})_3$, where silicon atoms replace some of the Al atoms in TiAl_3 to generate $\text{Ti}(\text{Al}, \text{Si})_3$ [39].

4.2 Relationship among heat input, IMCs, and mechanical properties

It is generally recognized that welding heat input plays an important role in the growth of IMCs. During the CMT Twin welding-brazing of Ti/Al dissimilar metals, the aluminum alloy melts and the titanium alloy remains in solid, forming a solid titanium-liquid aluminum reaction system. In theory, there are two important views on the formation of IMCs in solid alloy-liquid aluminum systems. One is that IMCs began to grow during the dissolution of a solid metal, and heat input affects the thickness of IMCs by affecting the diffusion rate and interfacial reaction rate [40]. Another view is that the IMCs formed during cooling and heat input influences IMCs by affecting atomic diffusion [41]. Both theories admit that diffusion is the most important factor controlling the growth of IMCs, and the diffusive mechanism of

particles during the solid–liquid phase interfacial reaction is a non-stationary diffusion process, which can be briefly described by referring to Fick’s second law for the diffusion of titanium atoms into the weld [9]:

$$\frac{\partial c}{\partial t} = D \frac{\partial^2 c}{\partial x^2}$$

where c is the concentration of Ti atoms, t is the diffusion time, x is the distance of Ti atoms relative to the interfacial

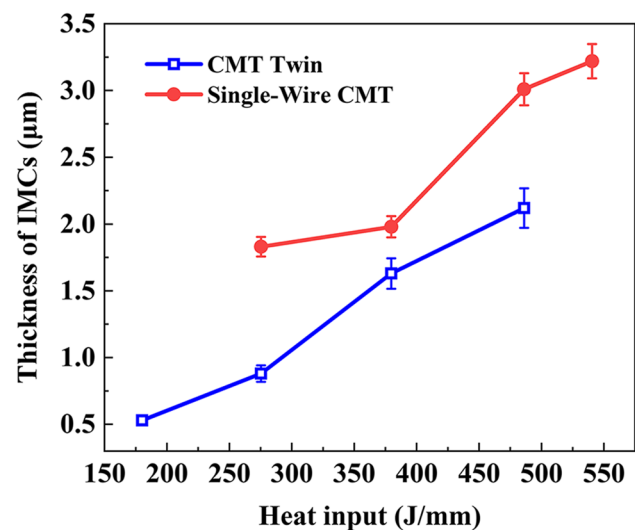
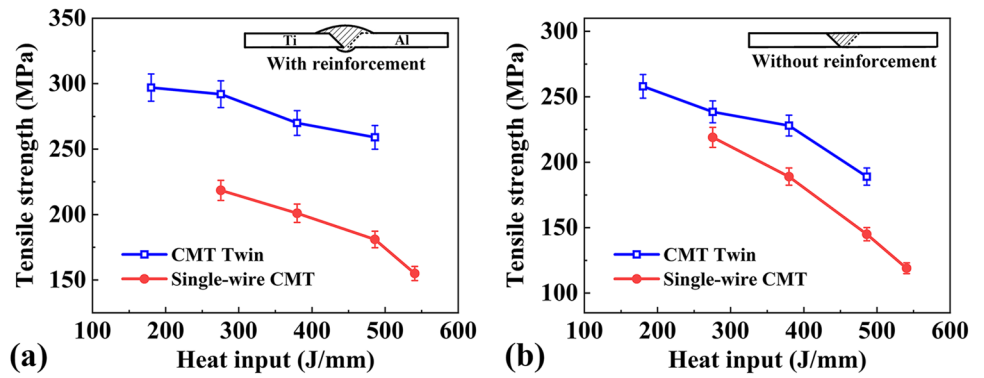


Fig. 6 Relationship between welding heat input and thicknesses of IMCs

Fig. 7 Relationship between joint strength and heat input: **a** with reinforcement, **b** without reinforcement



layer, and D is the diffusion coefficient. Assuming that the Ti atom content in the weld metal at the beginning is “ c_0 ,” the following derivation can be made:

$$c = c_0 - c_0 * \operatorname{erf}\left(\frac{x}{\sqrt{2Dt}}\right)$$

where $\operatorname{erf}(\beta)$ represents the value of the error function corresponding to different β values, due to the diffusion coefficient D :

$$D = D_0 \exp\left(-\frac{Q}{RT}\right)$$

D_0 is the diffusion constant determined by the diffusion mechanism, and R is the gas constant and is a constant value. T is the absolute temperature, and Q is the activation energy per mole of atomic diffusion. The higher the reaction temperature, the higher the welding heat input, and the more intense the diffusion movement of Ti atoms. The welding speed, wire feeding rate, and other process parameters determine the growth of IMCs by affecting the welding heat input. Some works have reported that the IMC thickness at the Al/Ti interface increases with increasing heat input in arc welding-brazing [14] and laser welding-brazing [42] processes. The results presented in Fig. 6 of this study are consistent with these results. A higher heat input indicates a higher interface temperature and a longer reaction time, which leads to a larger IMC thickness.

The strength of Ti/Al dissimilar joints mainly depends on the morphology and thickness of the interfacial IMCs [19, 43, 44]. The difference in the thermal expansion coefficient between 5083Al ($2.6 \times 10^{-5} \text{ }^\circ\text{C}^{-1}$) and TC4 ($7.9 \times 10^{-6} \text{ }^\circ\text{C}^{-1}$) will lead to the generation of residual stress, and the presence of brittle inclusions is prone to stress concentration under the influence of welding thermal stresses and other factors, which becomes the origin of fracture cracks. Under the influence of the inherent brittleness, the excessively thick IMC may not only spontaneously initiate fracture cracks under the action of residual stress but also provide a channel for crack propagation and aggravate the fracture trend of the joint. Therefore, to obtain a sound Al/Ti joint, the IMC thickness has to be kept to the lowest possible value [45].

4.3 Comparison of the single-wire CMT and CMT Twin processes

The CMT Twin can be used for high-speed welding under a relatively low heat input and avoid common defects such as undercuts and humps. According to the classical double ellipsoidal heat source model and a developed model for double-wire welding, the temperature field of the double-wire heat source is elongated along the welding direction, the temperature gradient during the welding process is small, the pool volume is increased, and the liquid metal can fully flow and wet the titanium alloy

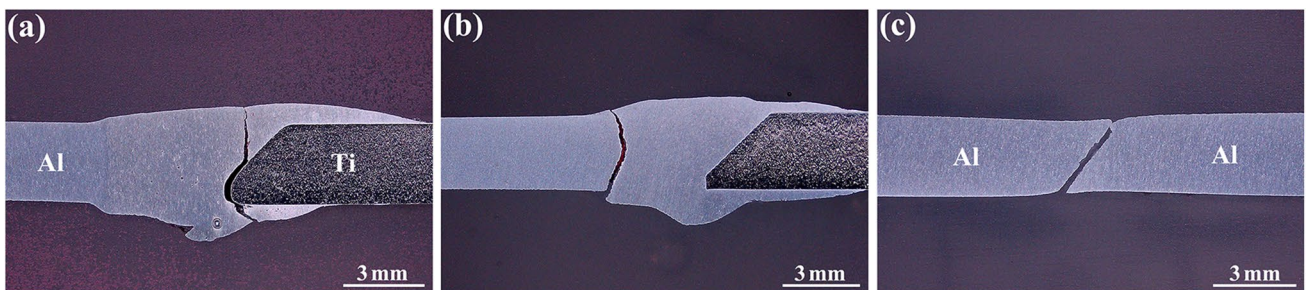


Fig. 8 Fracture positions of the joints by CMT Twin: **a** 259 MPa, **b** 295 MPa, **c** 297 MPa

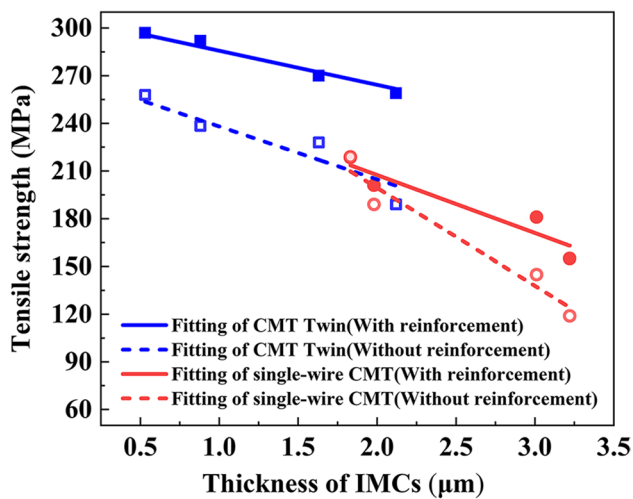


Fig. 9 Relationship between IMC thickness and joint strength

[46–48]. On the other hand, under the action of surface tension, the liquid metal flows from the center of the two heat sources to the edge of the molten pool at the same time, and the liquid convection is more stable, avoiding the appearance of the defects [49]. Thus, the CMT Twin welding speed can reach 2–3 times that of the conventional single-wire CMT, which is of great significance to realize low heat input, limit the growth of IMCs, and improve the joint strength.

Under the same heat input, the IMC of the CMT Twin joint is significantly thinner than that of the single-wire CMT, possibly attributed to the calculation equation of the heat input, the difference of interfacial thermal cycles, and the status of the welding pool. First, the heat input is calculated according to the linear energy formula $Q=UI/V$ without considering the thermal efficiency η , which has a different value between 0.5 and 0.8 depending on actual welding methods. In addition, for the two welding sources (single-wire CMT and CMT Twin), the temperature field shapes, temperature gradients during cooling, and welding pool agitation are different, which will affect the formation and growth of the IMCs, resulting in different IMC thicknesses.

For previous studies of the traditional single-wire CMT on Al/Ti joining, the thickness of IMC obtained by R. Cao was 5 μm , and the tensile strength of the joint was

199 MPa [32]. In this research, the strength of the single-wire CMT joint is 225 MPa with an IMC thickness of 1.83 μm , while the highest strength of the CMT Twin joint can be up to 297 MPa with a minimum IMC thickness of only 0.53 μm . The CMT Twin shows advantages over the single-wire CMT in terms of a higher welding speed, lower heat input, thinner IMC thickness, and higher joint strength.

5 Conclusions

A CMT Twin technique was applied to Al/Ti joining and obtained a sound joint. With the CMT Twin, the welding heat input and IMC thickness were successfully controlled, and the joint strength increased to a new level that equals the strength of the base aluminum. The following conclusions can be drawn:

- (1) By employing the CMT Twin on Al/Ti joining, the reasonable range of the welding heat input was extended and shifted to a negative direction compared with the single-wire CMT.
- (2) TEM analysis of the Al/Ti welding-brazing interface showed a dominant layer of $\text{Ti}(\text{Al}, \text{Si})_3$, which grew in a serrated pattern from the titanium alloy to the weld seam.
- (3) By using the CMT Twin on Al/Ti welding, the thickness of the IMC was controlled to a minimum value of 0.53 μm , and the corresponding maximum tensile strength of the joint was up to 297 MPa.
- (4) With decreasing heat input, the IMC thickness decreased, while the joint strength increased, and the fracture position transferred from the IMC layer to the base aluminum.
- (5) The CMT Twin shows advantages over single-wire CMT in terms of higher welding speed, lower heat input, thinner IMC thickness, and higher joint strength.

Funding The authors are thankful for the financial support provided by the National Natural Science Foundation of China (Grant No. 52005112, 51605263), Science and Technology Planning Project of Guangzhou City (Grant No. 201807010035, 201807010011), and Science and Technology Planning Project of Guangdong Academy of Sciences (Grant No. 2020GDASYL-20200402006, 2020GDASYL-20200302013).

Declarations

Conflict of interest The authors declare no competing interests.

Table 4 Fitting results of the strength variation

	CMT Twin with reinforcement	CMT Twin without reinforcement	Single-wire CMT with reinforcement	Single-wire CMT without reinforcement
Slope	-21.47	-33.29	-36.44	-61.51

References

- Stemper L, Tunes MA, Tosone R, Uggowitzer PJ, Pogatscher S (2022) On the potential of aluminum crossover alloys. *Prog Mater Sci* 124:100873
- Zhang XS, Chen YJ, Hu JL (2018) Recent advances in the development of aerospace materials. *Prog Aerosp Sci* 97:22–34
- Möller F, Thomy C, Vollertsen F (2012) Joining of titanium-aluminium seat tracks for aircraft applications system technology and joint properties. *Weld World* 56:108–114
- Zhou XF, Cao XB, Zhang F, Chen Z, Duan JA (2021) Effects of AlSi12 interlayer on microstructure and mechanical properties of laser welded 5A06/Ti6Al4V joints. *Weld World* 65:1389–1402
- Gadakh VS, Badheka VJ, Mulay AS (2021) Solid-state joining of aluminum to titanium: a review. *Proceedings of the Institution of Mechanical Engineers, Part L: J of Mater: Des App* 235:1757–1799.
- Jiang SY, Li SC, Zhang L (2013) Microstructure evolution of Al-Ti liquid-solid interface. *T Nonferr Metal Soc* 23:3545–3552
- Chaudhari R, Parekh R, Ingle A (2014) Reliability of dissimilar metal joints using fusion welding: a review. in: *International Conference on Machine Learning, Electrical and Mechanical Engineering*.
- Fronczek D, Wojewoda-Budka J, Chulist R, Sypien A, Korneva A, Szulc Z, Schell N, Zieba P (2016) Structural properties of Ti/Al clads manufactured by explosive welding and annealing. *Mater Des* 91:80–89
- Luo JG, Acoff VL (2000) Interfacial reactions of titanium and aluminum during diffusion welding. *Weld J* 79:239s–243s
- Fuji A, North TH, Kimura M, Ameyama K (1995) Effect of friction welding on characteristics of pure titanium/A5083aluminum alloy joint Report 1: Joint Mechanical Properties. *J Soc Mater Sci Japan* 44:188–192
- Kar A, Suwas S, Kailas SV (2018) Two-pass friction stir welding of aluminum alloy to titanium alloy: a simultaneous improvement in mechanical properties. *Mat Sci Eng: A* 733:199–210
- Geyer M, Vidal V, Pottier T, Boher C, Rezai-Aria F (2021) Investigations on the material flow and the role of the resulting hooks on the mechanical behaviour of dissimilar friction stir welded Al2024-T3 to Ti-6Al-4V overlap joints. *J Mater Process Tech* 292:117057
- Yu MR, Zhao HY, Xu F, Chen TJ, Zhou L, Song XG, Ma NS (2020) Influence of ultrasonic vibrations on the microstructure and mechanical properties of Al/Ti friction stir lap welds. *J Mater Process Tech* 282:116676
- Ma ZP, Wang CW, Yu HC, Yan JC, Shen HR (2013) The microstructure and mechanical properties of fluxless gas tungsten arc welding-brazing joints made between titanium and aluminum alloys. *Mater Des* 45:72–79
- Wei SZ, Li YJ, Wang J, Liu K, Zhang PF (2014) Microstructure and joining mechanism of Ti/Al dissimilar joint by pulsed gas metal arc welding. *Int J Adv Manuf Tech* 70:1137–1142
- Huang JK, Liu YL, Liu SE, Guan ZC, Yu XQ, Wu HS, Yu SR, Fan D (2021) Process of welding-brazing and interface analysis of lap joint Ti-6Al-4V and aluminum by plasma arc welding. *J Manuf Process* 61:396–407
- Nandagopal K, Kailasanathan C (2016) Analysis of mechanical properties and optimization of gas tungsten Arc welding (GTAW) parameters on dissimilar metal titanium (6Al-4V) and aluminium 7075 by Taguchi and ANOVA techniques. *J Alloy Compd* 682:503–516
- Li JZ, Sun QJ, Liu YB, Cai CW, Feng JC (2017) Cold metal transfer welding-brazing of pure titanium TA2 to aluminum alloy 6061–T6. *Adv Eng Mater* 19:1600494
- Chen SH, Li LQ, Chen YB, Dai JM, Huang JH (2011) Improving interfacial reaction nonhomogeneity during laser welding-brazing aluminum to titanium. *Mater Des* 32:4408–4416
- Tomashchuk I, Sallamand P, Cicala E, Peyre P, Grevey D (2015) Direct keyhole laser welding of aluminum alloy AA5754 to titanium alloy Ti6Al4V. *J Mater Process Tech* 217:96–104
- Tomashchuk I, Sallamand P, Méasson A, Cicala E, Duband M, Peyre P (2017) Aluminum to titanium laser welding-brazing in V-shaped groove. *J Mater Process Tech* 245:24–36
- Zhu ZT, Wang W, Li YX, Chen H (2019) Effect of laser-arc offset and laser-deviation angle on the control of a Ti-Al interlayer. *J Mater Process Tech* 271:336–345
- Wang T, Li XP, Zhang YY, Li HJ, Zhang BG, Feng JC (2017) Regulating the interfacial morphology of electron beam welded pure Ti/2024Al dissimilar joint. *J Mater Process Tech* 245:227–231
- Li P, Lei ZL, Zhang XR, Chen YB (2020) Influence of Si content on interfacial reactions and mechanical properties of dual-spot laser welded-brazed Ti/Al joints. *J Manuf Process* 56:950–966
- Malikov A, Vitoshkin I, Orishich A, Filippov A, Karpov E (2020) Effect of the aluminum alloy composition (Al-Cu-Li or Al-Mg-Li) on structure and mechanical properties of dissimilar laser welds with the Ti-Al-V alloy. *Opt Laser Tech* 126:106135
- Chang SY, Tsao LC, Lei YH, Mao SM, Huang CH (2012) Brazing of 6061 aluminum alloy/Ti-6Al-4V using Al-Si-Cu-Ge filler metals. *J Mater Process Tech* 212:8–14
- Lv SX, Cui QL, Huang YX, Jing XJ (2013) Influence of Zr addition on TIG welding-brazing of Ti-6Al-4V to Al5A06. *Mat Sci Eng: A* 568:150–154
- Dong KW, Kong J, Peng Y, Zhou Q, Wang KH (2020) A new strategy for high-strength joining of dissimilar materials. *J Mater Process Tech* 283:116724
- Li XF, Li CX, Cao ZL, Yang P (2020) The effect of Zn interlayer on microstructure and mechanical performance during TIG overlap welding-brazing of Al to Ti. *Mater Res Express* 7:026514
- Majumdar B, Galun R, Weisheit A, Mordike B (1997) Formation of a crack-free joint between Ti alloy and Al alloy by using a high-power CO₂ laser. *J Mater Sci* 32:6191–6200
- Zhang YF, Huang JH, Ye Z, Cheng Z, Yang J, Chen SH (2018) Influence of welding parameters on the IMCs and the mechanical properties of Ti/Al butt joints welded by MIG/TIG double-sided arc welding-brazing. *J Alloy Compd* 747:764–771
- Cao R, Sun JH, Chen JH (2013) Mechanisms of joining aluminium A6061–T6 and titanium Ti–6Al–4V alloys by cold metal transfer technology. *Sci Technol Weld Joi* 18:425–433
- Gao M, Chen C, Gu YZ, Zeng XY (2014) Microstructure and tensile behavior of laser arc hybrid welded dissimilar Al and Ti alloys. *Materials* 7:1590–1602
- Cui XP, Fan GH, Geng L, Wang Y, Huang LJ, Peng HX (2012) Growth kinetics of TiAl₃ layer in multi-laminated Ti-(TiB₂/Al) composite sheets during annealing treatment. *Mat Sci Eng: A* 539:337–343
- Sujata M, Bhargava S, Sangal S (1997) On the formation of TiAl₃ during reaction between solid Ti and liquid Al. *J Mater Sci Lett* 16:1175–1178
- He H, Zhao KP, Gou WQ, Qiao PB, Yuan EW (2021) Growth characterisation of TiAl₃ during initial period of hot dip aluminising on Ti6Al4V. *Trans IMF* 99:146–152
- Raman A, Schubert K (1965) On the constitution of some alloy series related to TiAl₃. II. Investigations in some T4–Al–Si and T4...6-in systems. *Z Metallk* 56:44–52
- Zhang CQ, Robson JD, Haigh SJ, Prangnell PB (2019) Interfacial segregation of alloying elements during dissimilar ultrasonic welding of AA6111 aluminum and Ti6Al4V titanium. *Metall Mater Trans A* 50:5143–5152

39. Sun QJ, Li JZ, Liu YB, Li BP, Xu PW, Feng JC (2017) Microstructural characterization and mechanical properties of Al/Ti joint welded by CMT method-assisted hybrid magnetic field. *Mater Des* 116:316–324
40. Dybkov VI (2013) *Solid State Reaction Kinetics*. IPMS publications, Kyiv
41. Ding ZY, Hu QD, Lu WQ, Sun SY, Xia MX, Li JG (2017) In situ observation on the formation of intermetallics compounds at the interface of liquid Al/solid Ni. *Scripta Mater* 130:214–218
42. Chen YB, Chen SH, Li LQ (2009) Effects of heat input on microstructure and mechanical property of Al/Ti joints by rectangular spot laser welding-brazing method. *Int J Adv Manuf Tech* 44:265
43. Takemoto T, Okamoto I (1988) Intermetallic compounds formed during brazing of titanium with aluminium filler metals. *J Mater Sci* 23:1301–1308
44. Chen SH, Li LQ, Chen YB, Huang JH (2011) Joining mechanism of Ti/Al dissimilar alloys during laser welding-brazing process. *J Alloy Compd* 509:891–898
45. Baqer YM, Ramesh S, Yusof F, Manladan S (2018) Challenges and advances in laser welding of dissimilar light alloys: Al/Mg, Al/Ti, and Mg/Ti alloys. *Int J Adv Manuf Tech* 95:4353–4369
46. Goldak J, Chakravarti A, Bibby M (1984) A new finite element model for welding heat sources. *Mater Trans B* 15:299–305
47. Dong KQ, Liu CY, Xiao QJ (2006) Study of heat source model for temperature field simulation in double wire welding processes. *Hot Working Technology* 35:49–52
48. Chen J, Han ZK, Wang L, Wu CS (2020) Influence of arc interactions on heat and mass transfer during a two-arc hybrid welding. *Int J Heat Mass Tran* 148:119058
49. Michie K, Blackman S, Ogunbiyi TB (1999) Twin-wire GMAW: process characteristics and applications. *Weld J* 78:31–34

Publisher's note Springer Nature remains neutral with regard to jurisdictional claims in published maps and institutional affiliations.